

A Transition in the Pairing Symmetry of the Electron-Doped Cuprates

John A. Skinta and Thomas R. Lemberger

Department of Physics, Ohio State University, Columbus, OH 43210-1106

T. Greibe and M. Naito

NTT Basic Research Laboratories, 3-1 Morinosato Wakamiya, Atsugi-shi, Kanagawa 243, Japan

(December 2, 2024)

We present measurements of the penetration depth, $\lambda^{-2}(T)$, in a series of $\text{Pr}_{2-x}\text{Ce}_x\text{CuO}_4$ and $\text{La}_{2-x}\text{Ce}_x\text{CuO}_4$ thin films at various doping levels, x . At low T , $\lambda^{-2}(T)$ is cubic in T at optimal and overdoping, and quadratic at underdoping. We propose that this signals a transition in pairing symmetry from d - to s -wave near optimal doping.

PACS numbers: 74.25.Fy, 74.76.Bz, 74.72.Jt

I. INTRODUCTION

A victory in the effort to understand the high- T_c superconductors has been the determination of the order parameter symmetry in the hole-doped cuprates. A variety of experiments [1–6] have demonstrated that h-doped cuprates possess a predominantly d -wave gap. In contrast, there is no consensus concerning order parameter symmetry in electron-doped cuprates. Phase-sensitive [7], ARPES [8], and some penetration depth [9,10] measurements on optimally doped $\text{Pr}_{2-x}\text{Ce}_x\text{CuO}_4$ (PCCO) and $\text{Nd}_{2-x}\text{Ce}_x\text{CuO}_4$ (NCCO) samples suggest d -wave pairing. Other penetration depth measurements [11,12] and the absence of a zero-bias conductance peak in tunnelling measurements [13,14] indicate s -wave superconductivity.

To date, experimental studies of e-doped cuprates have concentrated on optimally doped samples. To explore the doping dependence of e-doped cuprate properties and to resolve the pairing symmetry controversy, we present measurements of $\lambda^{-2}(T)$ in a series of PCCO and $\text{La}_{2-x}\text{Ce}_x\text{CuO}_4$ (LCCO) thin films at various dopings, x . The curvature near T_c and low- T magnitude of the superfluid density, $n_s(T) \propto \lambda^{-2}(T)$, depend strongly on doping. Furthermore, the T -dependence of $\lambda^{-2}(T)$ at low T changes with doping: $\lambda^{-2}(T)$ is cubic at optimal and overdoping, but quadratic at underdoping. We propose that this reveals a transition in pairing symmetry from d - to s -wave near optimal doping. Contradictory e-doped pairing symmetry results can thus be reconciled, if one assumes that nominally optimally doped samples that exhibit d -wave properties are in reality underdoped.

II. EXPERIMENTAL

The six e-doped films studied were prepared by molecular-beam epitaxy (MBE) on $12.7 \text{ mm} \times 12.7 \text{ mm} \times 0.35 \text{ mm}$ SrTiO_3 substrates as detailed elsewhere [15–17]. Table 1 summarizes important film parameters. The optimal PCCO film is film P2 from Ref. 12. The films are highly c -axis oriented, and their ab -plane resistivities, $\rho(T)$ – shown in Fig. 1 – are low.

We measure $\lambda^{-2}(T)$ with a two-coil mutual inductance technique described in detail elsewhere [18]. Films are centered between two coils each approximately 2 mm in diameter and 1 mm long. The sample is cooled to 1.6 K, and a current of ≤ 10 mA is driven at 50 kHz through the drive coil. As T slowly increases, the voltage induced in the pickup coil is measured continuously. The current density induced in the film is essentially uniform through its thickness. Because the coils are much smaller than the film, the applied field is concentrated near the center of the film and demagnetizing effects at the edges are irrelevant. Care is taken to ensure that the data are taken in the linear response regime.

The film's complex sheet conductivity, $\sigma(T)d = \sigma_1(T)d - i\sigma_2(T)d$ where d is the film thickness, is deduced from the measured mutual inductance. σ_1 is large enough to be detectable only near T_c . We define T_c and ΔT_c to be the temperature and full width of the peak in σ_1 . $\lambda^{-2}(T)$ is obtained from the imaginary part of the conductivity as $\lambda^{-2}(T) \equiv \mu_0\omega\sigma_2(T)$, where μ_0 is the magnetic permeability of vacuum. We take great pains to reduce the noise level at low T to approximately 0.2% of $\lambda^{-2}(0)$. Uncertainty in film thickness is the largest source of error in determination of $\lambda^{-2}(T)$. $\lambda(0)$ is known to $\sim 15\%$ accuracy in these films; however, this uncertainty does not impact the determination

of the T -dependence of $\lambda^{-2}(T)/\lambda^{-2}(0)$. As the films were grown in the same MBE apparatus on successive runs, we estimate the relative uncertainty in $\lambda(0)$ in each material to be $\sim 5\%$.

Measurement of $\sigma_1(T)$ is a stringent test of film quality, as inhomogeneities in any layer will broaden ΔT_c . Figure 2 displays $\sigma_1(T)$ measured at 50 kHz for each film. ΔT_c is typically ≤ 1 K, indicating excellent film quality. Structure in σ_1 is due to slight inhomogeneity. We believe that the small peak at 19.7 K in the overdoped LCCO data is due to a tiny bad spot at the film edge. No corresponding feature in $\lambda^{-2}(T)$ is apparent at 19.7 K (Fig. 3), indicating that this transition is unimportant to analysis of the data.

A few more words about sample quality and doping are in order. T_c is very weakly dependent on x near optimal doping, so using only T_c as a measure of doping level is dangerous. Resistivity is also a poor indicator, as literature values for $\rho(T_c^+) - \rho$ just above T_c – in optimal samples [19,20] are significantly higher than in our underdoped films. The intrinsic homogeneity problems of e-doped crystals [21,22] – Ce-poor surfaces and gradients in Ce content – make accurate determination of x in crystals additionally problematic. It is widely believed that e-doped films are superior to crystals, because the reduction process required to remove interstitial apical oxygen causes phase decomposition in bulk samples [15]. Superconducting LCCO is realizable *only* in films, as the large size of the La^{3+} ion makes bulk synthesis nearly impossible [17].

Figure 3 displays $\lambda^{-2}(T)$ for each film. Within experimental uncertainty, $\lambda^{-2}(0)$ is the same at optimal and overdoping and is a factor of 2 lower at underdoping. The upward curvature in $\lambda^{-2}(T)$ near T_c at optimal doping is enhanced with overdoping. Without offering an alternative explanation, we emphasize that the upward curvature seen in these films *is not* due to inhomogeneity, as the feature extends far below the sharp peak in σ_1 [23].

We have previously found that $\lambda^{-2}(T)$ in five optimal PCCO films is cubic at low T :

$$\lambda^{-2}(T) \sim \lambda^{-2}(0) \left[1 - \left(\frac{T}{T_0} \right)^C \right], \quad (1)$$

with C equal to 3 and $T_0 \approx 20$ K [12]. We were able to differentiate T^3 from T^2 by fitting only the first 5% drop in $\lambda^{-2}(T)$. The low T_c 's and T_0 's of under- and overdoped films make determination of low- T temperature dependence intrinsically more difficult. At under- and overdoping, accurate determination of low- T behavior requires expanding the fit range to include the first $\sim 10\%$ drop in $\lambda^{-2}(T)$. Extending our measurements to lower T would help alleviate this difficulty.

We now examine the low- T behavior of $\lambda^{-2}(T)$. $\lambda^{-2}(T)$ in optimal LCCO is cubic with $T_0 \approx 21.8$ K (Fig. 5, upper curve). Error bars represent experimental noise of 0.2%. It is reassuring that the anomalous T^3 dependence of $\lambda^{-2}(T)$ in optimal PCCO is corroborated by results from LCCO.

Figure 4 displays the first $\sim 8\%$ drop in $\lambda^{-2}(T)/\lambda^{-2}(0)$ in the overdoped films. Successive curves are offset by 0.02, and error bars represent 0.2% noise. Thin solid lines are best cubic fits ($C = 3$ in Eq. 1) and thin dotted lines are best quadratic fits ($C = 2$) to this data. T^3 fits to within 0.2%, while T^2 is numerically and visually inferior and lies well outside the noise in places. So, $\lambda^{-2}(T)$ is cubic at low T at overdoping, but with stronger curvature than at optimal doping (Table 1).

Figure 5 displays $\lambda^{-2}(T)/\lambda^{-2}(0)$ at low T at underdoping (lower curves), and the results of best quadratic (thin dotted lines) and cubic (thin solid) fits. Successive curves are offset for clarity, and error bars represent 0.2% noise. For PCCO, the cubic fit lies well outside of the experimental noise, and the quadratic fits exceedingly well. For LCCO, the quadratic fit is numerically and visually superior to the cubic fit, although we acknowledge that lower experimental T would strengthen this conclusion.

III. DISCUSSION

The strong dependence of $\lambda^{-2}(T)$ on doping in the e-doped cuprates is remarkable. We concentrate our discussion on the following: the suppression of $\lambda^{-2}(0)$ with underdoping, the increasing upward curvature of $\lambda^{-2}(T)$ near T_c with overdoping, and the transition in low- T behavior near optimal doping.

Within experimental uncertainty, $\lambda^{-2}(0)$ is the same at optimal and overdoping and is a factor of 2 lower at underdoping. The recently proposed d -density wave theory [24] predicts a very weak doping dependence of $n_s(0)$ above, and a sharp decrease in $n_s(0)$ below, a critical doping level, x_c [25]. Our films' behavior is qualitatively consistent with this prediction, but it is unknown what x_c is in e-doped cuprates.

The enhancement of upward curvature in $\lambda^{-2}(T)$ near T_c with increased doping is peculiar. $\lambda^{-2}(T)$ has downward curvature or is linear near T_c at underdoping, while upward curvature develops at optimal and overdoping. It is

unclear what the source of this feature is; however, we reemphasize that upward curvature *is not* associated with inhomogeneity.

Finally, we turn to the low- T behavior of $\lambda^{-2}(T)$. To our knowledge, the only theoretical explanation of $\lambda^{-2}(T) \propto T^3$ behavior is an s -wave order parameter with strong inelastic electron-phonon scattering [12,26]. The decrease in T_0 with overdoping indicates that scattering increases with x , although the transport scattering rate – estimated by $T_s \equiv \hbar\rho(T_c^+)/k_B\mu_0\lambda^2(0)$ – decreases with overdoping. In any case, $\lambda^{-2}(T)$ flatter than T^2 at low T has yet to be predicted or observed in a d -wave superconductor under any conditions (see Ref. 12), strengthening our s -wave interpretation. The quadratic behavior at underdoping is typical of d -wave superconductivity with disorder or nonlocal effects [27–29]. This change in low- T temperature dependence with doping indicates a transition in pairing symmetry in e -doped cuprates.

IV. CONCLUSION

We have presented measurements of $\lambda^{-2}(T)$ from 1.6 K through T_c in PCCO and LCCO films at various dopings. Film quality is demonstrably high, and film properties are reproducible. $\lambda^{-2}(0)$ is the same at optimal and overdoping and decreases by a factor of 2 at underdoping. Upward curvature in $\lambda^{-2}(T)$ near T_c develops at optimal doping and increases with overdoping. At low T , $\lambda^{-2}(T)$ is cubic at optimal and overdoping, and is quadratic at underdoping. T^3 behavior is consistent with an s -wave order parameter with strong inelastic scattering, while T^2 indicates d -wave superconductivity. This apparent transition in pairing symmetry reconciles contradictory literature results on e -doped cuprates, assuming that nominally optimally doped samples that exhibit d -wave characteristics are in fact underdoped.

V. ACKNOWLEDGEMENTS

This work was supported in part by DoE Grant DE-FG02-90ER45427 through the Midwest Superconductivity Consortium.

-
- [1] W.N. Hardy *et al.*, Phys. Rev. Lett. **70**, 3999 (1993).
 - [2] D.J. Van Harlingen, Rev. Mod. Phys. **67**, 515 (1995).
 - [3] D.A. Bonn and W.N. Hardy, in *Physical Properties of High Temperature Superconductors V*, edited by D.M. Ginsberg (World Scientific, Singapore, 1996).
 - [4] S. Kamal *et al.*, Phys. Rev. B **58**, R8933 (1998).
 - [5] C.C. Tsuei and J.R. Kirtley, Rev. Mod. Phys. **72**, 969 (2000).
 - [6] C.C. Tsuei and J.R. Kirtley, Physica (Amsterdam) **341-348C**, 1625 (2000).
 - [7] C.C. Tsuei and J.R. Kirtley, Phys. Rev. Lett. **85**, 182 (2000).
 - [8] N.P. Armitage *et al.*, Phys. Rev. Lett. **86**, 1126 (2001).
 - [9] J.D. Kokales *et al.*, Phys. Rev. Lett. **85**, 3696 (2000).
 - [10] R. Prozorov *et al.*, Phys. Rev. Lett. **85**, 3700 (2000).
 - [11] L. Alff *et al.*, Phys. Rev. Lett. **83**, 2644 (1999).
 - [12] J.A. Skinta *et al.*, submitted to Phys. Rev. Lett.
 - [13] S. Kashiwaya *et al.*, Phys. Rev. B **57**, 8680 (1998).
 - [14] L. Alff *et al.*, Phys. Rev. B **58**, 11197 (1998).
 - [15] M. Naito *et al.*, Physica (Amsterdam) **293C**, 36 (1997).
 - [16] M. Naito and H. Sato, Appl. Phys. Lett. **67**, 2557 (1995); H. Yamamoto *et al.*, Phys. Rev. B **56**, 2852 (1997).
 - [17] M. Naito and M. Hepp, Jpn. J. Appl. Phys. Lett. **39**, 485 (2000).
 - [18] S.J. Turneaure *et al.*, J. Appl. Phys. **79**, 4221 (1996); S.J. Turneaure *et al.*, *ibid.* **83**, 4334 (1998).
 - [19] P. Fournier *et al.*, Phys. Rev. Lett. **81**, 4720 (1998).
 - [20] J.D. Kokales *et al.*, Physica (Amsterdam) **341-348C**, 1655 (2000).
 - [21] A.R. Drews *et al.*, Physica (Amsterdam) **200C**, 122 (1992).
 - [22] E.F. Skelton *et al.*, Science **263**, 1416 (1994).

- [23] We have observed upward curvature in λ^{-2} near T_c before, but never at T below the fluctuation peak in σ_1 . We ascribe upward curvature with non-zero σ_1 to film inhomogeneity.
- [24] S. Chakravarty *et al.*, Phys. Rev. B **63**, 094503 (2001).
- [25] Q.-H. Wang *et al.*, cond-mat/0011398 (2000).
- [26] G.V. Klimovich *et al.*, JETP Lett. **53**, 399 (1991).
- [27] J.F. Annett *et al.*, in *Physical Properties of High Temperature Superconductors II*, edited by D.M. Ginsberg (World Scientific, Singapore, 1990).
- [28] P.J. Herschfeld and N. Goldenfeld, Phys. Rev. B **48**, 4219 (1993).
- [29] I. Kosztin and A.J. Leggett, Phys. Rev. Lett. **79**, 135 (1997).

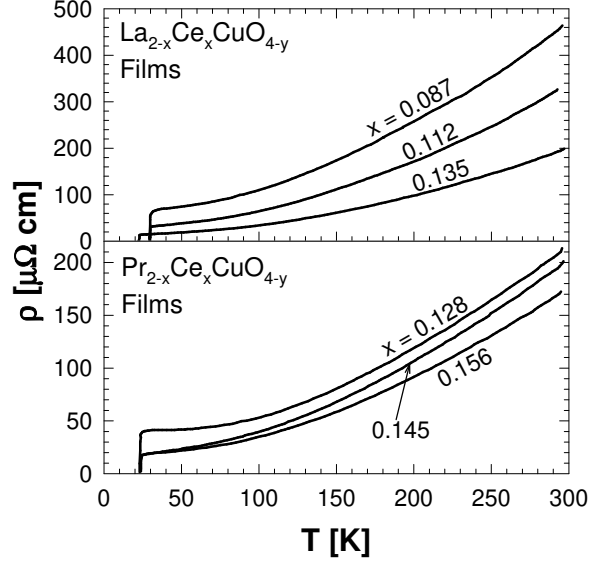


FIG. 1. ab -plane resistivities, $\rho(T)$, of six e-doped films. For resistivities just above T_c , see Table 1.

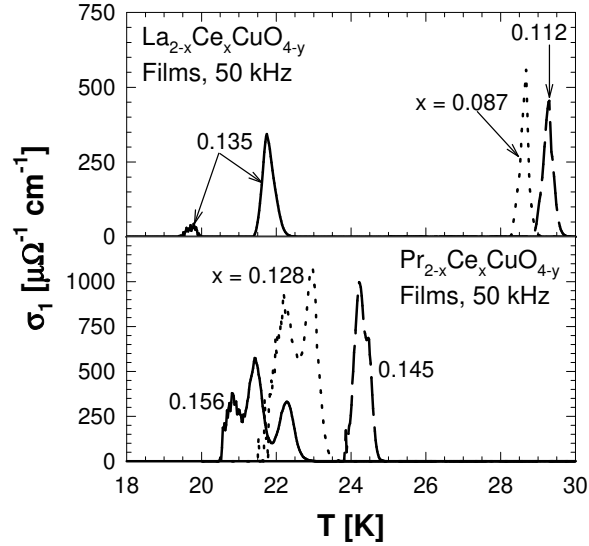


FIG. 2. $\sigma_1(T)$ at 50 kHz in six e-doped films. T_c and ΔT_c are temperature and full width of peak in σ_1 .

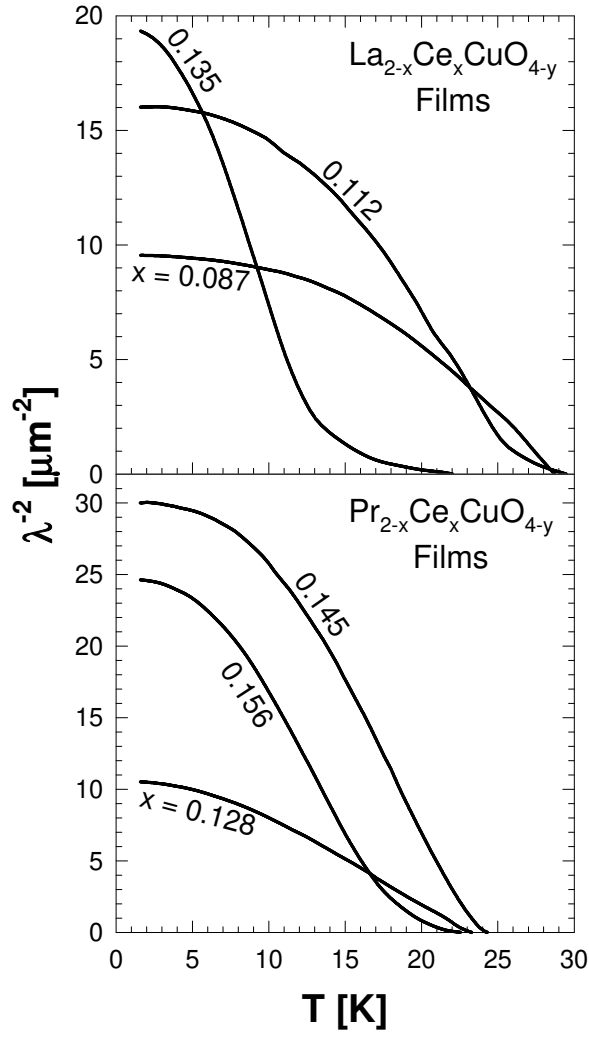


FIG. 3. $\lambda^{-2}(T)$ for various x in six e-doped films. Relative uncertainty in $\lambda^{-2}(0)$ in each material is $\sim 10\%$.

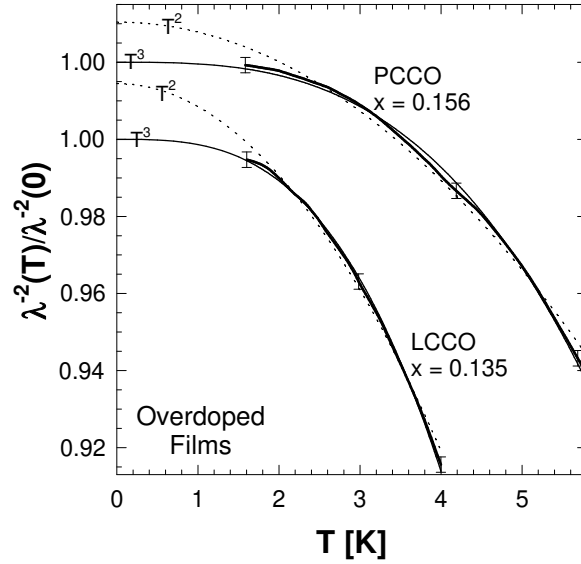


FIG. 4. First 8% drop in $\lambda^{-2}(T)/\lambda^{-2}(0)$ for overdoped films (thick lines), offset for clarity. Error bars represent experimental noise of 0.2%. Thin solid (dotted) lines are best cubic (quadratic) fits to $\lambda^{-2}(T)/\lambda^{-2}(0)$ over this range. Cubic fits are superior.

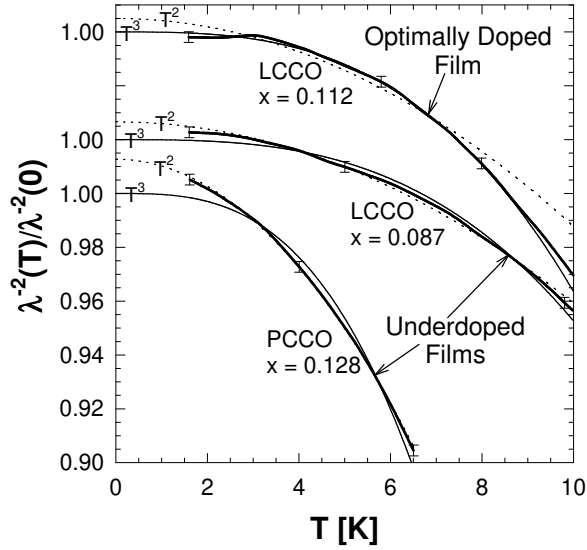


FIG. 5. $\lambda^{-2}(T)/\lambda^{-2}(0)$ at low T for optimal (upper curve) and underdoped (lower curves) films, offset for clarity. Error bars represent experimental noise of 0.2%. Thin solid (dotted) lines are best cubic (quadratic) fits to $\lambda^{-2}(T)/\lambda^{-2}(0)$ over this range. For optimal LCCO, the fit extends only to 8 K and is extrapolated to higher T . Optimal film is cubic, and underdoped films are quadratic, at low T .

TABLE I. Properties of six e-doped films. x is Ce doping and is known to ± 0.005 . d is film thickness. T_c and ΔT_c determined from location and full width of peak in σ_1 . T_0 is determined from best power-law fits to first 5 to 10% drop in $\lambda^{-2}(T)$. Absolute uncertainty in $\lambda^{-2}(0)$ is $\pm 15\%$.

Film	x	d [Å]	T_c [K]	ΔT_c [K]	T_0 [K]	$\lambda(0)$ [Å]	$\rho(T_c^+)$ [$\mu\Omega\text{cm}$]
underdoped LCCO	0.087	1250	28.7	0.8	24.6	3200	70
optimal LCCO	0.112	1250	29.3	0.9	21.8	2500	35
overdoped LCCO	0.135	1250	21.7	1.0	9.0	2300	20
underdoped PCCO	0.128	1000	22.5	1.8	13.9	3100	40
optimal PCCO	0.145	1000	24.2	1.0	19.1	1800	20
overdoped PCCO	0.156	1000	21.5	2.4	13.3	2000	20